

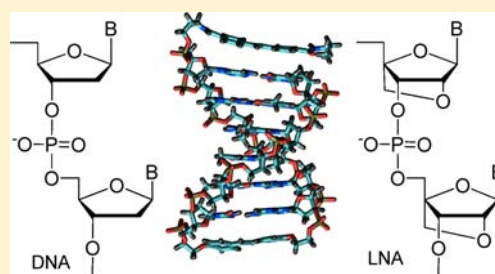
# Dynamics and Efficiency of Hole Transport in LNA:DNA Hybrid Diblock Oligomers

Arun K. Thazhathveetil, Josh Vura-Weis,<sup>†</sup> Anton Trifonov,<sup>‡</sup> Michael R. Wasielewski,\* and Frederick D. Lewis\*

Department of Chemistry and Argonne-Northwestern Solar Energy Research (ANSER) Center, Northwestern University, Evanston, Illinois 60208, United States

**S** Supporting Information

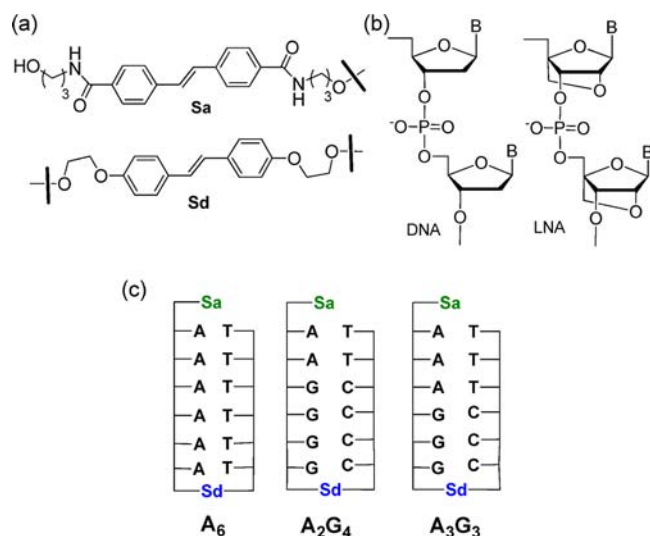
**ABSTRACT:** We report here the effect of replacing one or both of the purine or pyrimidine blocks of a diblock stilbene donor–acceptor capped hairpin with locked nucleic acid (LNA) bases on the dynamics and efficiency of hole transport. The structures of the DNA and LNA:DNA hybrids are tentatively assigned to B- or A-type structures on the basis of their circular dichroism spectra. Replacing the bases in either the A-block or the G-block of the diblock DNA hairpin with LNA bases results in a modest decrease in the base-to-base hopping rate constant and quantum yield for charge separation. Somewhat larger decreases are observed when all of the purine or pyrimidine bases are replaced by LNA bases.



Electron transfer in DNA continues to attract the attention of both experimental and theoretical scientists. It is now generally accepted that transport of positive charge (holes) over multiple base pairs in DNA occurs via a hole hopping mechanism, the rate of which is dependent upon the base sequence.<sup>1</sup> Several years ago, we introduced the use of stilbene donor–acceptor capped hairpins (Chart 1) for the investigation of the picosecond–nanosecond dynamics and efficiency of charge separation in DNA as a function of the duplex length and base sequence.<sup>2–7</sup> Our investigations of charge separation

in capped hairpins possessing poly(dA) sequences and diblock poly(dA):poly(dG) sequences (Chart 1c) provided rate constants of  $1.2 \times 10^9$  and  $4.3 \times 10^9$  s<sup>-1</sup> for reversible A-to-A and G-to-G hopping, respectively, values that are in excellent agreement with recent theoretical models for these hopping processes.<sup>8</sup> These rate constants are significantly faster than the values for alternating or random base sequences.<sup>5,9</sup> Thus, poly(G) provides the benchmark against which the dynamics of DNA hole transport measurements currently can be evaluated.<sup>9,10</sup>

**Chart 1. Structures of (a) the Stilbenes Sa and Sd, (b) DNA and LNA Dinucleotides, and (c) Capped Hairpins A<sub>6</sub>, A<sub>2</sub>G<sub>4</sub>, and A<sub>3</sub>G<sub>3</sub>**



Recently, there has been growing interest in determining the effects of alteration of the oligonucleotide bases or sugar–phosphate backbone on the dynamics of electron transfer. Okamoto et al. reported more efficient hole transport via a DNA wire containing size-expanded versus natural adenines;<sup>11</sup> however, hole transport dynamics were not determined. Kawai et al. investigated the dependence of hole transport kinetics in alternating (GX)<sub>n</sub> oligomers on ionization potential of the base X, where X is a natural or modified base.<sup>9</sup> They attributed changes in hole transport dynamics that occurred upon replacement of the base X to changes in HOMO energy gaps between adjacent bases in the hole transport pathway. We have suggested that enhanced hopping rates for poly(7-deazaadenine) versus adenine in a diblock purine system might be a consequence of increased conformational mobility resulting from the removal of the 7-amino group from the major groove.<sup>10,12</sup> Nuclear and solvent reorganization have been suggested as factors responsible for the slow rates of hole transport in DNA.<sup>13</sup>

Received: August 10, 2012

Published: September 7, 2012

Among the backbone modifications that have drawn attention as alternatives to the deoxyribose of DNA in studies of charge transport are the stretched deoxyribose backbone (Zip-DNA),<sup>14</sup> peptide nucleic acids (PNA),<sup>15,16</sup> and locked nucleic acids (LNA, Chart 1b).<sup>17,18</sup> Molecular dynamics (MD) simulations for Zip-DNA reveal enhanced intrastrand base stacking leading to predictions of rapid charge transport, which remain to be experimentally tested.<sup>14</sup> MD simulations of PNA duplexes indicate they are more flexible than DNA duplexes and thus predicted to undergo more rapid charge transfer.<sup>15</sup> A recent experimental study of charge transfer in two PNA duplexes found more rapid charge transfer in the more flexible structure.<sup>16</sup> MD simulations for a LNA:DNA duplex and for a structurally related A-DNA duplex by Ivanova et al. revealed reduced intrastrand electronic coupling but increased inter-strand coupling for certain base sequences when compared to DNA.<sup>17,19</sup> This led to the prediction that it should be possible to design a LNA-modified sequence with a high propensity for hole transport. Kawai et al. recently reported the results of an experimental study of hole transport in alternating (GA)<sub>6</sub> and (GT)<sub>6</sub> sequences in which these sequences and/or the complementary strand are replaced with LNA bases.<sup>18</sup> Without considering the prior work of Ivanova et al.,<sup>17,20</sup> they state “LNA modification completely suppressed the charge transfer through DNA in the time range of <100 μs,” even though their own data for LNA:DNA duplexes are not fully in agreement with this conclusion.

We report here our investigation of the dynamics and efficiency of hole transport in LNA:DNA diblock hairpins (Table 1). Circular dichroism spectroscopy is used as a convenient method to screen for changes from B- to A-type DNA structures. We find that the rate constant for G-to-G hopping in LNA G-blocks (<sup>L</sup>G<sub>n</sub>) is  $\sim 3 \times 10^9$  s<sup>-1</sup>, a factor of only 1.3 slower than that for a DNA G-block. The rate constant

**Table 1. Quantum Yields for Charge Separation ( $\Phi_{cs}$ ) and Charge Separation Times ( $\tau_{cs}$ ) for LNA:DNA and DNA Capped Hairpins<sup>a</sup>**

LNA:DNA <sup>b</sup>	$\Phi_{cs}$	$\tau_{cs}$ , ns	DNA <sup>c</sup>	$\Phi_{cs}$	$\tau_{cs}$ , ns
<sup>L</sup> A <sub>6</sub>	≥0.02	≥10	A <sub>6</sub>	0.09	9.0
<sup>L</sup> A <sub>2</sub> G <sub>4</sub>	0.24	1.5	A <sub>2</sub> G <sub>4</sub>	0.32	1.0
<sup>L</sup> A <sub>3</sub> G <sub>3</sub>	0.14	4.7	A <sub>3</sub> G <sub>3</sub>	0.30	0.91
<sup>L</sup> A <sub>4</sub> G <sub>2</sub>	≥0.06	≥10	A <sub>4</sub> G <sub>2</sub>	0.15	1.4
A <sub>2</sub> <sup>L</sup> G <sub>4</sub>	0.28	1.6			
A <sub>3</sub> <sup>L</sup> G <sub>3</sub>	0.26	1.9			
A <sub>2</sub> <sup>L</sup> G <sub>6</sub>	0.23	5.6	A <sub>2</sub> G <sub>6</sub>	0.24	4.2
A <sub>2</sub> <sup>L</sup> G <sub>8</sub>	≥0.19	≥10	A <sub>2</sub> G <sub>8</sub> <sup>e</sup>	0.24	6.0
<sup>L</sup> A <sub>2</sub> <sup>L</sup> G <sub>4</sub>	0.17	1.9			
<sup>L</sup> A <sub>3</sub> <sup>L</sup> G <sub>3</sub>	≥0.09	9.0			
T <sub>2</sub> <sup>L</sup> C <sub>4</sub>	0.31	1.7			
<sup>L</sup> T <sub>2</sub> <sup>L</sup> C <sub>4</sub>	0.24	2.5			
<sup>L</sup> (A <sub>2</sub> G <sub>4</sub> ) <sup>d</sup>	≥0.13	≥10			

<sup>a</sup>Structures of selected capped hairpins are shown in Chart 1. Data shown are averages of two or more measurements for solutions of ca. 50 μM hairpin at 25 °C in phosphate buffer (10 mM phosphate, 0.1 M NaCl, pH 7.2). Errors are ca. 10% except when reported as lower bounds for which errors are 25%. <sup>b</sup>Superscript L denotes LNA bases in the following block of nucleotides. Complementary strand has DNA bases except where noted. <sup>c</sup>Data for DNA capped hairpins are from ref 6. <sup>d</sup>All bases in both strands of <sup>L</sup>(A<sub>2</sub>G<sub>4</sub>) are LNA bases. <sup>e</sup>Values estimated from the data in ref 6.

for A-to-A hopping in short LNA A-blocks (<sup>L</sup>A<sub>n</sub>) is also slightly slower than that in a DNA A-block. Slower hopping rate constants are accompanied by lower quantum yields for charge separation. The effects of replacing all of the purine bases, all of the pyrimidine bases, or all of the bases in both strands with LNA bases have also been investigated. Our results are consistent with the conclusion of Ivanova and co-workers that intrastrand electronic coupling in A-type DNA is slightly smaller than that in B-type DNA.<sup>17,20</sup>

## RESULTS

**Synthesis and Spectra of Capped Hairpins.** Capped hairpins possessing LNA purine bases <sup>L</sup>A or <sup>L</sup>G or pyrimidine bases <sup>L</sup>T or <sup>L</sup>C were prepared and characterized by the methods previously described for the A<sub>n</sub> and A<sub>n</sub>G<sub>m</sub> hairpins (see the Supporting Information).<sup>6</sup> The UV spectra of the LNA-containing conjugates are similar to those of their DNA analogues, consisting of two broad bands centered near 335 and 260 nm.<sup>3</sup> The former is assigned to the lowest energy  $\pi,\pi^*$  transition of the two stilbenes and the latter to the overlapping absorption of the nucleobases and higher energy transitions of the stilbenes. Representative spectra for hairpins A<sub>6</sub> (Chart 1c) and <sup>L</sup>A<sub>6</sub> shown in Figure 1 are essentially superimposable.

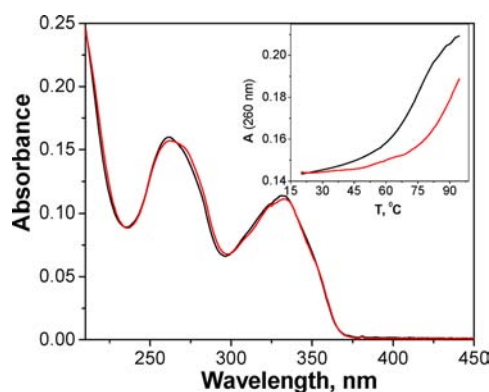


**Figure 1.** Normalized UV spectra of hairpins A<sub>6</sub> (black) and <sup>L</sup>A<sub>6</sub> (red) (ca. 2.5 μM in phosphate buffer, 10 mM phosphate, 0.1 M NaCl, pH 7.2). Inset shows 260 nm thermal dissociation profiles.

Thermal dissociation profiles determined at 260 nm are provided in the inset to Figure 1. The first derivative of the profile for A<sub>6</sub> provides a value of  $T_m = 75.1$  °C, whereas the profile for <sup>L</sup>A<sub>6</sub> shows incomplete melting upon heating to 90 °C. Thus, the higher thermal stability previously reported for LNA:DNA duplex and hairpin systems also is observed for the capped hairpins.<sup>21,22</sup> The fluorescence spectra of hairpins A<sub>6</sub> and <sup>L</sup>A<sub>6</sub> are similar; however, the spectrum of <sup>L</sup>A<sub>6</sub> is somewhat more structured and more intense than that of A<sub>6</sub> (Figure S1).

The CD spectra for several DNA and LNA:DNA hairpins are shown in Figure 2. The CD spectrum of hairpin A<sub>6</sub> (Figure 2a) is similar to those of a capped hairpin having Sa chromophores at both ends and to a closely related Sa–Sd capped hairpin.<sup>2,23</sup> The long wavelength regions of the CD spectra of DNA hairpins A<sub>6</sub> and A<sub>3</sub>G<sub>3</sub> (Figure 2b) display positive and negative bands attributed to long-range exciton coupling (EC) between the two stilbene chromophores. The sign and amplitude of the EC-CD spectra are determined by distance and dihedral angle between the electronic transition dipoles of the two stilbene chromophores.<sup>23</sup> Replacement of the purine strand of these DNA hairpins with an all-LNA purine strand results in

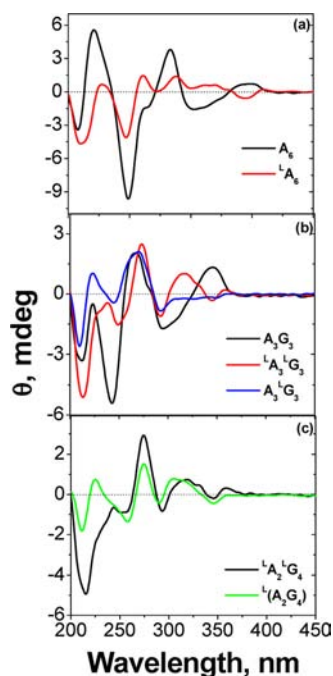


**Figure 2.** CD spectra of capped hairpins (ca. 5  $\mu\text{M}$  in phosphate buffer, 10 mM phosphate, 0.1 M NaCl, pH 7.2) (a)  $A_6$  and  $^L A_6$ , (b)  $A_3G_3$ ,  $A_3^L G_3$ , and  $^L A_3^L G_3$ , and (c)  $^L A_2^L G_4$  and  $^L(A_2G_4)$ .

inversion of the sign of the EC-CD spectrum, indicative of a substantial change in the relative geometry of the two stilbenes. Replacement of one-half of the purines in  $A_3G_3$  with LNA bases results in near total loss of intensity of the stilbene EC-CD band (Figure 2b).

The CD spectra of the LNA:DNA hairpins in the short wavelength region (200–300 nm) (Figure 2) are also dependent upon both the number and the location of LNA bases. The diblock LNA:DNA hairpins  $^L A_3^L G_3$  and  $^L A_2^L G_4$  have a strong negative band near 215 nm (Figure 2a), characteristic of LNA:DNA duplexes and, more generally, of A-type DNA.<sup>22,24,25</sup> This band is weaker in  $^L A_6$  and in the all-LNA duplex  $^L(A_2G_4)$  (Figure 2a,c). Stronger CD spectra are observed for complete versus partial substitution of the purines in  $A_3G_3$  (Figure 3b), as previously reported by Nielsen et al. for partially versus fully modified LNA:RNA duplexes.<sup>24</sup> In general,

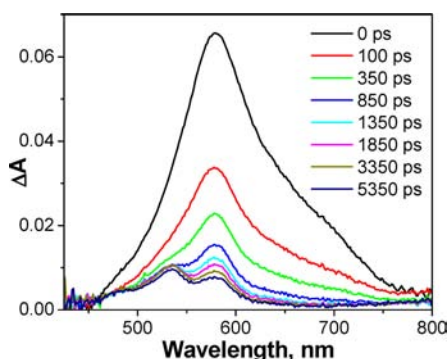


**Figure 3.** Transient spectra of  $^L A_2^L G_4$ . The trace at 0 ps represents the locally excited singlet state ( $^1S_a$ ) immediately after laser excitation. The absorption maxima of the  $S_a^{*-}$  radical anion and the  $S_d^{*+}$  radical cation are at 575 and 535 nm, respectively.

the CD spectra of LNA:DNA hairpins display more maxima and minima than do their DNA analogues.

#### Dynamics and Efficiency of Charge Separation.

Femtosecond (fs) time-resolved transient absorption spectra in aqueous solution were obtained as previously described for  $A_6$  and  $A_n G_m$  DNA hairpins (see the Supporting Information).<sup>6</sup> The transient absorption spectra shown in Figure 3 for  $^L A_2^L G_4$  are typical of our spectra for LNA-containing hairpins and are similar to those previously reported for DNA hairpins. Plots of the ratio of 525 nm/575 nm transient absorbance for several LNA containing conjugates are shown in Figure 4a,b. A short

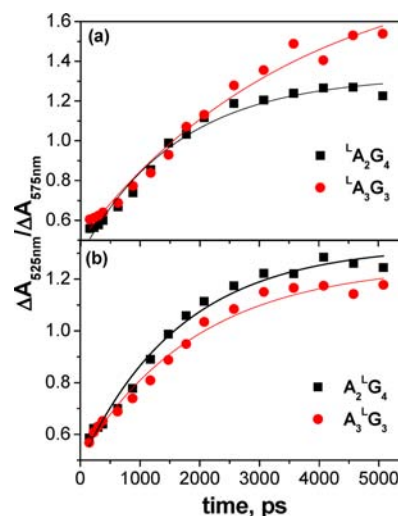


**Figure 4.** Plot of  $\Delta A_{525\text{nm}}/\Delta A_{575\text{nm}}$  versus time for (a)  $^L A_2 G_4$  and  $^L A_3 G_3$  and (b)  $A_2^L G_4$  and  $A_3^L G_3$  sequences.

induction period (<0.5 ns) is observed prior to the rise of the 525 nm/575 nm ratio for LNA-containing hairpins having an  $^L A_n$  or  $^L T_n$  base sequence adjacent to the Sa hole donor (Figure 4a), the length of which increases with  $n$ . No such induction period is observed for the LNA-containing hairpins having an  $A_n$  sequence adjacent to Sa (Figure 4b). Superimposed on these plots are first-order kinetic fits, which provide the charge separation times ( $\tau_{cs}$ ) reported in Table 1 along with previously reported data for DNA capped hairpins.<sup>6</sup> No attempt was made to account for the induction periods in these fits. The transient spectra do not decay on the time scale of our measurements, indicative of the formation of long-lived charge-separated states.

Quantum yields for charge separation ( $\Phi_{cs}$ ) are estimated as previously described for  $A_6$  and  $A_n G_m$  DNA hairpins by comparing the integrated band intensities of the transient absorption spectra at long delay times with that for a capped hairpin having a single A–T base pair separating Sa and Sd ( $\Phi_{cs} = 1$ ).<sup>26</sup> Values of  $\Phi_{cs}$  for LNA-modified hairpins are reported in Table 1 along with previously reported values for DNA diblock capped hairpins.<sup>6</sup> In cases where the 525 nm/575 nm band intensity ratio is still rising at 6 ns, the value of  $\Phi_{cs}$  is reported as a lower bound.

In the case of  $^L A_6$ , the value of  $\Phi_{cs}$  is  $\sim 0.02$ , near the detection limit of our apparatus, and the value of  $\tau_{cs}$  is too slow to measure ( $\geq 10$  ns). For the series of hairpins  $^L A_2 G_4$ ,  $^L A_3 G_3$ , and  $^L A_4 G_2$ , the value of  $\tau_{cs}$  increases from 1.5 to >10 ns, whereas the value of  $\tau_{cs}$  for the corresponding DNA hairpins increases only from 1.0 to 1.4 ns. The decrease in the values of  $\Phi_{cs}$  for this series of LNA hairpins is also larger than that for the DNA hairpins. When the backbone of the G track is locked as



opposed to that of the A tract, the change from native DNA is less pronounced. Values of  $\Phi_{cs}$  for these diblock systems are also only slightly smaller than those for the corresponding DNA hairpins and are only modestly dependent upon the length of the duplex.

Replacement of all of the DNA purine bases with LNA bases was investigated for the hairpins  ${}^L A_2{}^L G_4$  and  ${}^L A_3{}^L G_3$ . The values of  $\tau_{cs}$  are longer than those of the hairpins in which only the A-block or G-block has been replaced with LNA bases, and the values of  $\Phi_{cs}$  are somewhat smaller. Replacement of the DNA pyrimidine bases with LNA bases was investigated for the hairpins  $T_2{}^L C_4$  and  ${}^L T_2{}^L C_4$ . The values of  $\tau_{cs}$  and  $\Phi_{cs}$  for pyrimidine replacement are similar to those for purine replacement. Finally, replacement of all of the purine and pyrimidine bases with LNA bases was investigated for the hairpin  ${}^L(A_2G_4)$ . The value of  $\tau_{cs}$  is longer than that for the  $A_2G_4$  LNA:DNA duplexes having either the purine or the pyrimidine strand replaced with LNA bases.

## DISCUSSION

**Spectra and Structure of LNA:DNA Hairpins.** The structures of stilbene-linked DNA hairpins have been well-documented by means of X-ray crystallography and solution  ${}^1H$  NMR structure determination, both of which support the formation of stable B-DNA structures in which the stilbene linker is  $\pi$ -stacked with the neighboring base pair.<sup>27,28</sup> Molecular dynamics simulations and CD spectroscopy of the stilbene-DNA conjugate  $A_6$  are consistent with the formation of a capped hairpin structure in which the capping group is  $\pi$ -stacked with the neighboring base pair.<sup>29</sup> A snapshot of a minimized structure obtained from a molecular dynamics simulation is shown in Figure 5. In this structure, the two stilbenes are approximately parallel to each other and perpendicular to the helical axis, allowing the observation of

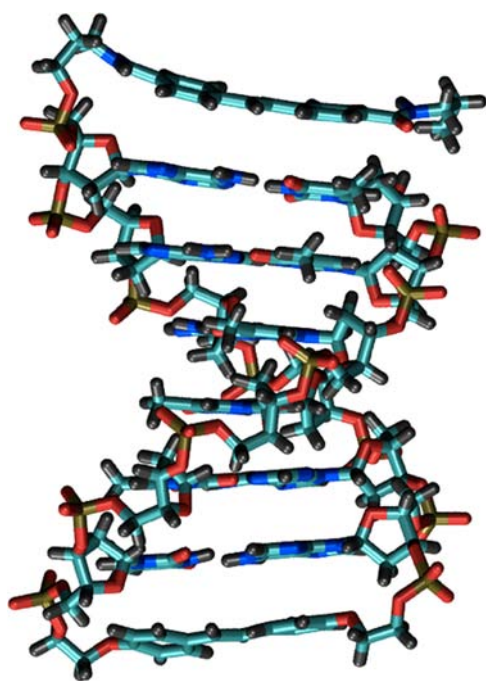


**Figure 5.** Minimized structure for the capped hairpin  $A_6$  obtained from a molecular dynamics simulation. The Sa capping group is at the top of the structure, and the Sd linker is at the bottom.

exciton coupled circular dichroism (EC-CD) between identical Sa chromophores separated by as many as 11 A–T base pairs.<sup>23</sup> The CD spectra of the DNA hairpins  $A_6$  and  $A_3G_3$  (Figure 2) both have moderately intense positive and negative bands at long wavelengths ( $>300$  nm) resulting from exciton coupling between their stilbene chromophores. Replacement of all of the purine bases with LNA bases in these hairpins causes an inversion in the sign of these bands, indicative of a substantial change in the relative geometries of the stilbene transition dipole moment vectors. When only one-half of the DNA purine bases are replaced in  $A_3{}^L G_3$ , the long wavelength CD bands vanish, consistent with formation of a structure that is one-half DNA and one-half LNA:DNA.

Comparison of the short-wavelength region of the CD spectra of the DNA and LNA:DNA hairpins (Figure 2) shows dominant negative peaks at ca. 250 nm for the former and 210 nm for the latter.<sup>22</sup> These and other differences in the CD spectra are consistent with a change in structure from B-type for the DNA hairpins to an A-type for the LNA:DNA hybrids. We assume that the differences in structure between the DNA and LNA:DNA hairpins occur primarily within the base pair domains and that the stilbenes remain  $\pi$ -stacked with the adjacent base pairs in both A- and B-type structures.

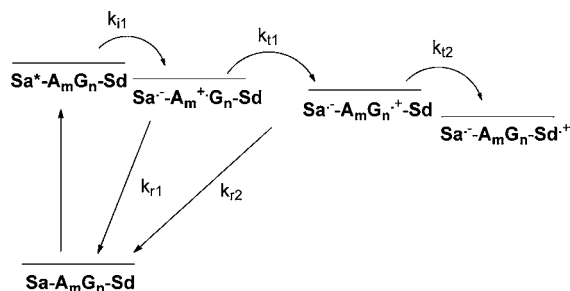
The molecular dynamics simulation reported for a 9-mer LNA:DNA duplex having a mixed-base sequence is also consistent with an A-type structure,<sup>19</sup> whereas an NMR study of the same duplex is suggestive of a geometry intermediate between A- and B-type.<sup>24</sup> The minimized structures for LNA:DNA and LNA:RNA duplexes have nonlinear helical axes;<sup>19,24</sup> hence, it is unlikely that the two stilbenes in a LNA:DNA hairpin are approximately parallel to each other as they are in the B-DNA capped hairpin (Figure 5). Thus, the sign and amplitude of the stilbene EC-CD spectra in the LNA:DNA hybrids cannot be simply correlated with the dihedral angle between the stilbene electronic transition dipole moments, as is possible for the B-DNA hairpins.<sup>23</sup> No information is currently available pertaining to the solution structure of all-LNA duplexes. The crystal structure of a short LNA duplex is strongly influenced by coordination with cobalt hexamine.<sup>30</sup>

Several theories have been advanced for the greater thermodynamic stability of LNA:DNA versus DNA duplexes. Among these are the entropic advantage of duplex formation with the conformationally more rigid bicyclic ribose analogue and more favorable base stacking in the hybrid duplex.<sup>21,22</sup> Enhanced base stacking was suggested to be responsible for enhanced photodimerization in the dinucleotide  $T_pT$  and in DNA hairpins containing a single TT step, when the TT step is replaced by LNA bases.<sup>31</sup> However, intrastrand purine–purine (A–A, G–G, G–A) base stacking is more extensive for B-type versus A-type DNA.<sup>32</sup> Ivanova and co-workers note that the substantial translation along the long axis of the base pairs in A-DNA “leads to an effective overlap between the bases of the two complementary strands.”<sup>20</sup>

**Dynamics and Efficiency of Hole Transport.** We previously investigated the dynamics and efficiency of hole transport in stilbene donor–acceptor capped hairpins having homopurine (poly(A) or poly(G)) or diblock purine ( $A_mG_n$ ) base sequences separating the donor and acceptor (Chart 1).<sup>6</sup> Rate constants for base-to-base hole transport in poly(G) sequences are larger than those in poly(A) sequences ( $4.3 \times 10^9$  vs  $1.2 \times 10^9$  s<sup>-1</sup>, respectively). This difference may be a consequence of specific solvation of A-tracts as well as the

higher energy HOMO orbitals for G versus A. Higher quantum yields for charge separation are observed in diblock systems having short A-blocks consisting of 2 or 3 A–T base pairs followed by G-blocks of variable length than in homopurine systems having the same total number of base pairs.<sup>6</sup> Enhanced charge separation efficiency in diblock systems is attributed to the lower oxidation potential of G versus A, which serves to inhibit charge return from the G block to the A block on the nanosecond time scale of our experiments (Scheme 1).<sup>6</sup>

**Scheme 1. Mechanism for Charge Separation in an  $A_nG_m$  Diblock Purpurine Capped Hairpin**



Replacement of the A-block bases with LNA bases results in even slower A-block hole transport, as reflected in the increase in  $\tau_{cs}$  for the LNA:DNA hairpins  ${}^L A_6$ ,  ${}^L A_2G_4$ ,  ${}^L A_3G_3$ , and  ${}^L A_4G_2$  versus their DNA analogues (Table 1). Slower A-to-A hole hopping in hairpins having A-block bases replaced with LNA bases allows A-block charge recombination to compete more effectively with A-to-G hole transport (Scheme 1,  $k_{r1}$  vs  $k_{t1}$ ), thus accounting for the decrease in  $\Phi_{cs}$  with increasing length of the LNA A-block. In view of the complex nature of charge return, charge recombination, and charge transport within the short A-blocks of these DNA and LNA:DNA diblock purine systems, it is not possible to dissect a rate constant for A-to-A hole hopping in LNA A-blocks from our data. However, a conservative estimate would place an upper bound of a factor of 2 on the difference in hopping rates for LNA versus DNA A-blocks.

Values of  $\tau_{cs}$  for the DNA diblock systems  $A_2G_4$ ,  $A_2G_6$ , and  $A_2G_8$  increase from 1.0 to 6.0 ns, and the value of  $\Phi_{cs}$  decreases from 0.32 to 0.24 with increasing length of the G-block.<sup>6</sup> As we previously observed, each incremental G-block base requires an additional hopping step and thus delays the hole arrival time.<sup>6</sup> However, once the total number of base pairs is greater than four, charge recombination no longer is competitive with hole transport (Scheme 1,  $k_{r2} < k_{t2}$ ), and the quantum yield becomes independent of the number of base pairs in the G-block. Replacement of the G-block bases with LNA bases in the series  $A_2{}^L G_4$ ,  $A_2{}^L G_6$ , and  $A_2{}^L G_8$  results in only slightly slower and less efficient charge separation (smaller  $\Phi_{cs}$ ) than is observed with DNA bases (Table 1). This observation also applies to the diblock purine system  $A_3{}^L G_3$  and  $T_2{}^L C_4$  in which the pyrimidines complementary to the G-block have been replaced by LNA bases.

Assuming that the charge separation time for the DNA A-block is similar for the LNA:DNA and DNA diblock purine hairpins, the increased charge separation times for the LNA:DNA diblock hairpins can be attributed to slower traversal of the LNA versus DNA G-block. Because the transit time for an  $A_2$  block is much shorter (ca. 39 ps) than that for either a LNA or a DNA  $G_6$  or  $G_8$  block, the G-to-G base

hopping rate constant can be estimated from the value of  $\tau_{cs}$  ( $k_{hop} \approx N^2/2\tau_{cs}$ , where  $N$  is the number of hops and  $\tau_{cs}$  is the traversal time for the diblock purine).<sup>33</sup> The resulting value of  $k_{hop} \approx 3.2 \times 10^9 \text{ s}^{-1}$  is only slightly smaller than the value of  $4.3 \times 10^9 \text{ s}^{-1}$  for G-to-G hopping in a long DNA G-block.<sup>7</sup>

The values of  $\tau_{cs}$  for hairpins  ${}^L A_2{}^L G_4$ ,  ${}^L A_3{}^L G_3$ , and  ${}^L T_2{}^L C_4$ , in which all of the purines or pyrimidines have been replaced with LNA bases, are somewhat longer than those for the hairpins in which only the A-block or G-block has been replaced by LNA bases (Table 1). This result is consistent with a small decrease in the rate constant for hole transport in both the A-block and the G-block of the diblock hairpin upon replacement of either DNA purine or pyrimidine bases with LNA bases. The increase in  $\tau_{cs}$  for these hairpins is accompanied by a decrease in  $\Phi_{cs}$ . The reduction in  $\Phi_{cs}$  for the LNA:DNA hairpins  ${}^L A_2{}^L G_4$  and  ${}^L A_3{}^L G_3$  having all of their purine bases replaced versus the DNA hairpin is approximately equal to the sum of the reduction in  $\Phi_{cs}$  values for the hairpin with only the A-block replaced and the reduction in  $\Phi_{cs}$  values for the hairpin with only the G-block replaced. Thus, hole transport in one of the two diblock segments is independent of the presence or absence of LNA bases in the other segment.

Finally, the effect of replacing all of the DNA bases in both hairpin strands with LNA bases was investigated for the hairpin  $A_2G_4$ . The value of  $\tau_{cs}$  for  ${}^L(A_2G_4)$  was too long to measure with our femtosecond apparatus ( $\geq 10$  ns), but is clearly longer than that for hairpins in only the purine or pyrimidine bases are replaced by LNA bases ( $\tau_{cs} = 1.9$  and 2.5 ns, respectively, Table 1). The increase in  $\tau_{cs}$  and concomitant decrease in  $\Phi_{cs}$  are indicative of a slower hole hopping rate for the all-LNA hairpin than for LNA:DNA hybrid hairpins. The crystal structure of the cobalt hexamine complex of an all-LNA duplex has been reported to have enhanced intrastrand base stacking when compared to an RNA duplex;<sup>30</sup> however, the solution structure in the absence of the strongly coordinating cobalt hexamine has not been reported. In fact, the weaker negative 210 nm band in our CD spectrum of  ${}^L(A_2G_4)$  versus  ${}^L A_2{}^L G_4$  (Figure 2c) suggests to us that there is less intrastrand base stacking in the all-LNA duplex than in a LNA:DNA duplex.

## CONCLUDING REMARKS

The results of our investigation establish that replacement of either the purine or the pyrimidine bases with LNA bases in a stilbene-capped diblock hairpin result in only a modest decrease (<2-fold) in the rate constants for A-to-A or G-to-G hole hopping. This decrease in rate constant is manifested in the directly measured increase in charge separation time ( $\tau_{cs}$ ). We note that values of  $\tau_{cs}$  in  $A_2{}^L G_n$  diblock systems continue to increase with the addition of each additional base pair between the Sa hole donor and Sd hole trap, but that values of  $\Phi_{cs}$  are not sensitive to the length of the G-track, as is the case for DNA diblock systems.<sup>6</sup> Thus, we would again caution against the use of quantum yields, or worse yet relative yields, as surrogates for rate constants. This practice persists despite our warnings, as in a recent comparative study of strand cleavage efficiency in DNA, RNA, and LNA:DNA hybrids.<sup>34</sup>

The CD spectra for the LNA:DNA hairpins are consistent with a change in structure from B-type to A-type upon replacement of all of the purine or pyrimidine bases in one strand with LNA bases. Replacement of the purine bases in only the A- or G-block of the diblock purines results in values of  $\tau_{cs}$  and  $\Phi_{cs}$  intermediate between those for the DNA hairpins and those of the LNA:DNA hairpins. Our results are consistent

with the studies by Ivanova and co-workers of the structures and electronic couplings between base pairs in A-type versus B-type DNA and LNA:DNA hybrids.<sup>17,20</sup> These workers report somewhat smaller electronic coupling between base pairs possessing stacked purines in A- versus B-type DNA. They also investigated the effect of structural fluctuations on the electronic coupling matrix elements and concluded that they are not perturbed significantly on the nanosecond time scale of base-to-base hole transport by the rigidity of the LNA:DNA duplexes.

Our conclusion that hole transport dynamics are only slightly slower in LNA:DNA duplexes than in DNA is seemingly at odds with the recently reported conclusion of Kawai et al. that "LNA modification completely suppressed the charge transfer through DNA in the time range of  $<100 \mu\text{s}$ ."<sup>18</sup> These workers investigated the dynamics of charge transport in alternating (GA)<sub>6</sub> and (GT)<sub>6</sub> DNA, LNA:DNA, and all-LNA duplexes on the time scale  $10^5$ – $10^8 \text{ s}^{-1}$  by means of nanosecond laser flash photolysis. Kinetic modeling of hole arrival times provides rate constants for a single G–A–G hole transfer step of  $3.8 \times 10^7 \text{ s}^{-1}$  for DNA and  $6.0 \times 10^5 \text{ s}^{-1}$  for an LNA:DNA hybrid, a rate ratio of 38. Because G–A–G hole transfer is a tunneling process, it would be expected to be slower and more sensitive to small changes in electronic coupling than the G-to-G hopping rates studied in our hairpin systems. Curiously, these workers observed similar rates for G–T–G hole transport in DNA and LNA:DNA hybrids ( $7.0$  and  $4.0 \times 10^5 \text{ s}^{-1}$ ).<sup>18</sup> In fact, G–T–G hole transfer is almost as fast as G–A–G hole transfer in LNA:DNA hybrids! A plausible explanation for this seeming anomaly can be found in the increased overlap between bases of the complementary strands of the LNA:DNA hybrid, as noted by Ivanova.<sup>17</sup> Thus, increased interstrand G–A electronic coupling could compensate for poor intrastrand coupling in the (GT)<sub>6</sub> LNA:DNA hybrid. No such interstrand purine–purine coupling is possible for the (GA)<sub>6</sub> hybrid.

In conclusion, the effect of replacement of DNA bases with LNA bases in LNA:DNA hybrids is dependent upon the base sequence and mechanism for hole transport. The effect is small, less than a factor of 2, for intrastrand A-to-A and G-to-G hopping in our diblock purine hairpin systems and also for G–T–G transport, and somewhat larger, a factor of 38, for G–A–G transport investigated by Kawai et al.<sup>18</sup> Only in the case of all-LNA duplexes are slower G-to-G hopping rates (Table 1) and suppression of G–A–G transport observed.<sup>18</sup> Presumably, the solution structure of the all-LNA duplex (currently unknown) differs from the A-type structure of the LNA:DNA duplex and provides less electronic coupling between base pairs than does A- or B-type DNA. A detailed understanding of hole transport in LNA:DNA and all-LNA duplexes will require more precise knowledge of their solution structure, which to date is available only for a single mixed base 9-mer LNA:DNA hybrid.<sup>24</sup> In the absence of reliable NMR structures, molecular dynamics simulations provide the best source of information about structure.<sup>19</sup> Ivanova et al. have suggested on the basis of such simulations that it should be possible to design a sequence with a high propensity for hole transfer along an LNA-modified helix.<sup>17</sup> Our A<sub>2</sub><sup>L</sup>G<sub>n</sub> diblock hairpins that have values of  $\Phi_{\text{cs}}$  and  $\tau_{\text{cs}}$  that are only slightly smaller than those for their all-DNA analogues (Table 1) provide an approach to this objective.

## ■ ASSOCIATED CONTENT

### 📄 Supporting Information

Materials and methods, and characterization of conjugates ( $m/z$  and  $T_m$  values, UV, fluorescence, and CD spectra). This material is available free of charge via the Internet at <http://pubs.acs.org>.

## ■ AUTHOR INFORMATION

### Corresponding Author

[fdl@northwestern.edu](mailto:fdl@northwestern.edu)

### Present Addresses

<sup>†</sup>Department of Chemistry, University of California at Berkeley, Berkeley, California 94720, United States.

<sup>‡</sup>Department of Physics, Sofia University, 5 James Bourchier Boulevard, BG-1164 Sofia, Bulgaria.

### Notes

The authors declare no competing financial interest.

## ■ ACKNOWLEDGMENTS

We thank Martin McCullagh for providing the image used in Figure 5. This work was supported by the Chemical Sciences, Geosciences, and Biosciences Division, Office of Basic Energy Sciences, DOE under grant nos. DE-FG02-96ER14604 (F.D.L.) and DE-FG02-99ER14999 (M.R.W.).

## ■ REFERENCES

- (1) (a) Schuster, G. B., Ed. *Long-Range Charge Transfer in DNA, I and II*; Springer: New York, 2004; Vols. 236 and 237. (b) Wagenknecht, H. A. *Charge Transfer in DNA*; Wiley-VCH: Weinheim, 2005. Genereux, J. C.; Barton, J. K. *Chem. Rev.* **2010**, *110*, 1642.
- (2) Lewis, F. D.; Wu, Y.; Zhang, L.; Zuo, X.; Hayes, R. T.; Wasielewski, M. R. *J. Am. Chem. Soc.* **2004**, *126*, 8206.
- (3) Lewis, F. D.; Zhu, H.; Daublain, P.; Fiebig, T.; Raytchev, M.; Wang, Q.; Shafirovich, V. *J. Am. Chem. Soc.* **2006**, *128*, 791.
- (4) Lewis, F. D.; Zhu, H.; Daublain, P.; Cohen, B.; Wasielewski, M. R. *Angew. Chem., Int. Ed.* **2006**, *45*, 7982.
- (5) Lewis, F. D.; Daublain, P.; Cohen, B.; Vura-Weis, J.; Shafirovich, V.; Wasielewski, M. R. *J. Am. Chem. Soc.* **2007**, *129*, 15130.
- (6) Vura-Weis, J.; Wasielewski, M. R.; Thazhathveetil, A. K.; Lewis, F. D. *J. Am. Chem. Soc.* **2009**, *131*, 9722.
- (7) Conron, S. M. M.; Thazhathveetil, A. K.; Wasielewski, M. R.; Burin, A. L.; Lewis, F. D. *J. Am. Chem. Soc.* **2010**, *132*, 14388.
- (8) (a) Blaustein, G. S.; Lewis, F. D.; Burin, A. L. *J. Phys. Chem. B* **2010**, *114*, 6732. (b) Steinbrecher, T.; Koslowski, T.; Case, D. A. *J. Phys. Chem. B* **2008**, *112*, 16935.
- (9) Kawai, K.; Hayashi, M.; Majima, T. *J. Am. Chem. Soc.* **2012**, *134*, 4806.
- (10) Thazhathveetil, A.; Trifonov, A.; Wasielewski, M.; Lewis, F. D. *J. Am. Chem. Soc.* **2011**, *133*, 11485.
- (11) Okamoto, A.; Tanaka, K.; Saito, I. *J. Am. Chem. Soc.* **2003**, *125*, 5066.
- (12) Ganguly, M.; Wang, F.; Kaushik, M.; Stone, M. P.; Marky, L. A.; Gold, B. *Nucleic Acids Res.* **2007**, *35*, 6181.
- (13) (a) Venkatramani, R.; Keinan, S.; Balaeff, A.; Beratan, D. N. *Coord. Chem. Rev.* **2011**, *255*, 635. (b) Siritwong, K.; Voityuk, A. A. *WIREs Comput. Mol. Sci.* **2012**, *2*, 780.
- (14) Balaeff, A.; Craig, S. L.; Beratan, D. N. *J. Phys. Chem. A* **2011**, *115*, 9377.
- (15) Hatcher, E.; Balaeff, A.; Keinan, S.; Venkatramani, R.; Beratan, D. N. *J. Am. Chem. Soc.* **2008**, *130*, 11752.
- (16) Wierzbinski, E.; de Leon, A.; Yin, X.; Balaeff, A.; Davis, K. L.; Reppireddy, S.; Venkatramani, R.; Keinan, S.; Ly, D. H.; Madrid, M.; Beratan, D. N.; Achim, C.; Waldeck, D. H. *J. Am. Chem. Soc.* **2012**, *134*, 9335.



- (17) Ivanova, A.; Jezierski, G.; Rosch, N. *Phys. Chem. Chem. Phys.* **2008**, *10*, 414.
- (18) Kawai, K.; Hayashi, M.; Majima, T. *J. Am. Chem. Soc.* **2012**, *134*, 9406.
- (19) Ivanova, A.; Rösch, N. *J. Phys. Chem. A* **2007**, *111*, 9307.
- (20) Ivanova, A.; Shushkov, P.; Rösch, N. *J. Phys. Chem. A* **2008**, *112*, 7106.
- (21) Wengel, J.; Petersen, M.; Frieden, M.; Koch, T. *Lett. Pept. Sci.* **2004**, *10*, 237.
- (22) Bruylants, G.; Bocconcelli, M.; Snoussi, K.; Bartik, K. *Biochemistry* **2009**, *48*, 8473.
- (23) Lewis, F. D.; Zhang, L.; Liu, X.; Zuo, X.; Tiede, D. M.; Long, H.; Schatz, G. S. *J. Am. Chem. Soc.* **2005**, *127*, 14445.
- (24) Nielsen, K. E.; Rasmussen, J.; Kumar, R.; Wengel, J.; Jacobsen, J. P.; Petersen, M. *Bioconjugate Chem.* **2004**, *15*, 449.
- (25) Kaur, H.; Arora, A.; Wengel, J.; Maiti, S. *Biochemistry* **2006**, *45*, 7347.
- (26) For details see ref 5.
- (27) Egli, M.; Tereshko, V.; Mushudov, G. N.; Sanishvili, R.; Liu, X. Y.; Lewis, F. D. *J. Am. Chem. Soc.* **2003**, *125*, 10842.
- (28) Tuma, J.; Tonzani, S.; Schatz, G. C.; Karaba, A. H.; Lewis, F. D. *J. Phys. Chem. B* **2007**, *111*, 13101.
- (29) Grozema, F. C.; Tonzani, S.; Berlin, Y. A.; Schatz, G. C.; Siebbeles, L. D. A.; Ratner, M. A. *J. Am. Chem. Soc.* **2008**, *130*, 5157.
- (30) Eichert, A.; Behling, K.; Betzel, C.; Erdmann, V. A.; Fürste, J. P.; Förster, C. *Nucleic Acids Res.* **2010**, *38*, 6729.
- (31) (a) Desnous, C.; Babu, B. R.; Moriou, C.; Mayo, J. U. O.; Favre, A.; Wengel, J.; Clivio, P. *J. Am. Chem. Soc.* **2008**, *130*, 30.  
(b) Hariharan, M.; McCullagh, M.; Schatz, G. C.; Lewis, F. D. *J. Am. Chem. Soc.* **2010**, *132*, 12856.
- (32) Konorov, S. O.; Schulze, H. G.; Addiso, C. J.; Haynes, C. A.; Blades, M. W.; Turner, R. F. B. *Open Spectrosc. J.* **2009**, *3*, 9.
- (33) Bar-Haim, A.; Klafter, J. *J. Chem. Phys.* **1998**, *109*, 5187.
- (34) Wenge, U.; Wengel, J.; Wagenknecht, H.-A. *Angew. Chem., Int. Ed.* **2012**, DOI: 10.1002/anie.201204901.